Magnetic Prussian Blue Nanoparticles as Novel Theranostic Agents for Cancer

Shraddha Kale

B.E. in Biomedical Engineering, June 2013, Mumbai University

A Thesis submitted to

The Faculty of
The School of Engineering and Applied Science
of The George Washington University
in partial fulfillment of the requirements
for the degree of Master of Science

May 15, 2016

Thesis directed by

Rohan Fernandes
Principal Investigator, Children's National Medical Center

Jason Zara
Associate Professor of Engineering and Applied Science

Dedication

To my parents: for their love, guidance, support, and patience.

Abstract of Thesis

Magnetic Prussian Blue Nanoparticles as Novel Theranostic Agent for Cancer

Theranostic nanoparticles simultaneously possess therapeutic and diagnostic capabilities. These nanoparticles offer the potential for more sensitive diagnoses and improved treatment results in human diseases, using a single platform. In the past, Prussian blue nanoparticles were synthesized and were used independently for imaging and therapy applications in the field of cancer[4-8]. Inspired by the potential for improved outcomes using theranostic nanoparticles, we have developed a single theranostic nanoparticle platform that integrates both imaging and therapy capabilities. The objective of this paper is to synthesize composite, core shell magnetic gadolinium Prussian blue nanoparticles that function as excellent MRI contrast agents in both T1 and T2-weighted sequences and as photo-thermal therapy agents. The application of these nanoparticles would be for biomedical imaging, diagnostic and therapeutic on a nanoscale. The nanoparticles can be combined with medical imaging for detecting tumor sites in the body and also provide less invasive and more precise means for curing Neuroblastoma cancers.

Table of Contents

List of Figures

List of Tables

Chapter 1 – INTRODUCTION

1.1 Cancer is a serious health problem

The word cancer is a term used to describe a collection of related diseases[1]. Cancer can start anywhere in the body and causes the body's cells to divide in an unstoppable manner and spread into surrounding tissues[4]. Normally, healthy human cells grow and divide to form new cells before they grow old or become damaged. However, cancer develops because old and damaged cells become abnormal and produce new cells or undergo division even when not required[3]. These extra cells grow in to a mass of cells known as tumors[1,2,3]. According to the American Cancer Society a total of 589,430 Americans died of cancer in 2015, corresponding to about 1,600 deaths per day[2,4]. Malignant tumors have the capability to spread and invade the healthy tissues, whereas benign tumors do not spread but can become quite large and affect body functions[5]. Cancer is a genetic disease and can be caused by the changes in the genes that control cell functions[7,8].

1.2 Conventional Therapy and Limitations

According to the National Cancer Institute, there are more than 100 types of cancers, evenly classified by the organs and tissues, in which cancer cells grow abnormally[1,10,11]. Years of intense research and billions of dollars have been invested to increase the knowledge of the cause and biology of cancer which has led to the development of many improved treatment strategies[3,4,62]. Currently the primary treatments for cancer are surgery, chemotherapy and radiation[4]. When possible, surgery is often used to remove the

tumor. However, a major limitation of surgery is that in some cases, the entire tumor cannot be removed and can lead to spread of the disease[9]. A second treatment option is chemotherapy, where anti-cancer drugs are injected into the vein and pass through the bloodstream to reach and destroy cancer cells[2,4,14]. This treatment can be used before or after surgery Radiation therapy is also used to apply high energy radiation to kill the cancer cells[14]. Usually, radiation therapy is used in combination with chemotherapy or surgery to treat cancer. Current cancer therapies are largely limited by their inability to bypass biological barriers, nonspecific delivery and poor biodistribution of drugs, ineffectiveness against metastatic disease and drug resistance of cancer[18,62,63].

1.3 Nanoparticles used to diagnose and treat these tumors

The application of nanotechnology to cancer therapy has the potential to overcome these challenges by enabling the alteration in the synthesize of these particles for more precise and specific navigation in the body[10]. Nanotechnology in cancer treatment offers exciting possibilities that include the possibility of destroying cancerous tumors with minimally invasive procedures, reducing damage to the surrounding tissues and organs, along with enhancing detection of the cancer cells[11]. Most nanotechnology development is in a development stage with efforts to make these treatments easily available for the patients[12,13]. Nanoparticles facilitate properties like smaller size range (10 nm-1000 nm) that are easy to extravasate into the tumors with impoverished vasculature and the ability to combine the detection and therapy functionality, offering the potential for improved outcomes in cancer patients[17].

1.4 Theranostic Nanoparticles

The term theranostic nanoparticles refers to particles that can be used for therapy and detection of cancer cells[4,25]. These nanoparticles provide sensitive diagnoses and improved treatment of cancer cells using a single unique platform[16,17]. Theranostic nanoparticles have the potential for advanced capabilities including sustained, controlled release; targeted delivery and multimodality diagnosis[4]. The ability to determine the size of the tumor and also to treat the tumor using the same tool provides significant advantages over current cancer treatments[16-19]. Multiple imaging modalities have been implemented into a single nanotheranostic design by incorporating for enhanced diagnostic and therapy of cancer[60-61]. Various platforms like gold nanoshells, carbon nanotubes and fullerenes (CNTs), semiconductor materials and various metals oxide nanoparticles have been investigated for cancer imaging applications[52,62]. The limitations with these nanotheranostic agents are their associated toxicity as well as the fact that these nanoparticle platforms are expensive to synthesize and often use potentially harmful radiations like computed tomography (CT) for tumor detection[24-26]. Hence there is an urgent need to develop improved theranostic agents to overcome these limitations. The magnetic gadolinium Prussian blue theranostic nanoparticles developed in this work will potentially allow radiation-free detection with minimal invasive treatment procedures for tumor detection and therapy. Also these nanoparticles will be easy and inexpensive to synthesize[13]. In addition, Prussian blue and iron oxide nanoparticles are FDA approved and hence are safe for human consumption[5-10]. This suggests that the combination of the two has a strong possibility of also being very safe.

1.5 Theranostic Nanoparticles for Pediatric Cancer

There is an urgent need to develop less invasive and radiation free theranostic nanoparticles[11,12]. Magnetic gadolinium Prussian blue nanoparticles do not subject the patient to potentially harmful radiation that could have long term effects on the human body. These composite nanoparticles act as excellent T1- and T2 – weighted MRI contrast agents. T1 weighting typically gives the best images with gadolinium because of their dominant contribution to the magnitude of the signal for T1 images. In comparison, iron oxide particles tend to have much larger effect on the T2 weighted images[57-59]. Also, these magnetic gadolinium Prussian blue nanoparticles can be photothermally heated to ablate tumor cells and potentially shrink the tumors [6,7,8]. In this thesis, I have chosen Neuroblastoma cancer as the target model because of the high risk and difficulty for treatment. Neuroblastoma is the third most common pediatric cancer and the most common extracranial solid tumor in children accounting for 15% of cancer-related deaths in the pediatric age group[1-2]. The different treatments for this model of cancer include surgery, chemotherapy and radiation therapy, but there are downsides to these treatment options[3]. Hence there is a crucial need to develop a novel theranostic agent that could be used to diagnose and treat these cancers.

1.6 Magnetic Gadolinium Prussian Blue Nanoparticles (Fe_3O_4@GdPb) as Theranostic Agents

In this project, we have synthesized core shell composite Magnetic Gadolinium Prussian Blue nanoparticles (Fe_3O_4@GdPb) as a theranostic nanoparticles, which could be used for imaging as well as for therapy of cancer. The core of these nanoparticles is an iron oxide nanoparticle which is an excellent contrast agent for T2. The shell of these

composite nanoparticles consists of gadolinium Prussian blue nanoparticles, which can be used as T1- weighted contrast agents. Additionally, Prussian blue nanoparticles can be used for photothermal therapy of the tumor cells. Hence this composite nanoparticle allows us to develop a single nanoparticle that could be used for imaging as well as therapy using a single platform. Also, as mentioned previously, both iron oxide and Prussian blue nanoparticles are FDA approved and hence are safe for human consumption[5-8].

1.7 Prussian blue nanoparticles:

Prussian blue is an ancient dye that was serendipitously synthesized in the early 18th century[5]. Prussian blue is comprised of colloidal nanoparticles that are made up of mixed valance iron hexacyanoferrate with the generalized formula AFeIII[FeII(CN)6].yH2O (where y . 1–5 and A is a monovalent cation such as K+, Na+ or NH4+)[5]. Previously, these nanoparticles were used for laser induced photothermal therapy of tumor cells[5-7]. These nanoparticles have the capability of converting the light energy into heat energy at the near infrared region (NIR). Using this effect, these nanoparticles can be injected into a tumor and irradiated with a low power NIR laser, which in turn causes the ablation of tumor cells and shrinkage of the tumor[5-8].

1.8 Iron oxide Gadolinium Prussian blue nanoparticles (Fe_3O_4@GdPb):

The overall goal of this thesis is to synthesize a composite nanoparticle that offer the potential for more sensitive diagnoses and improved treatment results in human diseases, using a single platform. We have composed a core shell theranostic nanoparticle by

growing a nanoshell of Gadolinium Prussian blue nanoparticle around a magnetic iron oxide core (Fe_3O_4@GdPb). Additionally, Prussian blue and Iron oxide nanoparticles are approved by the U.S Food and Drug Administration[6,18]. The iron oxide core is an excellent T2 MRI contrast agent. The gadolinium present in the shell of the composite nanoparticle is a T1 MRI contrast agent. The Prussian blue nanoparticles have the capability of absorbing light at the visible near infrared region and photothermally converting the light energy into heat energy. These composite particles provide efficient MRI- guided photothermal therapy.

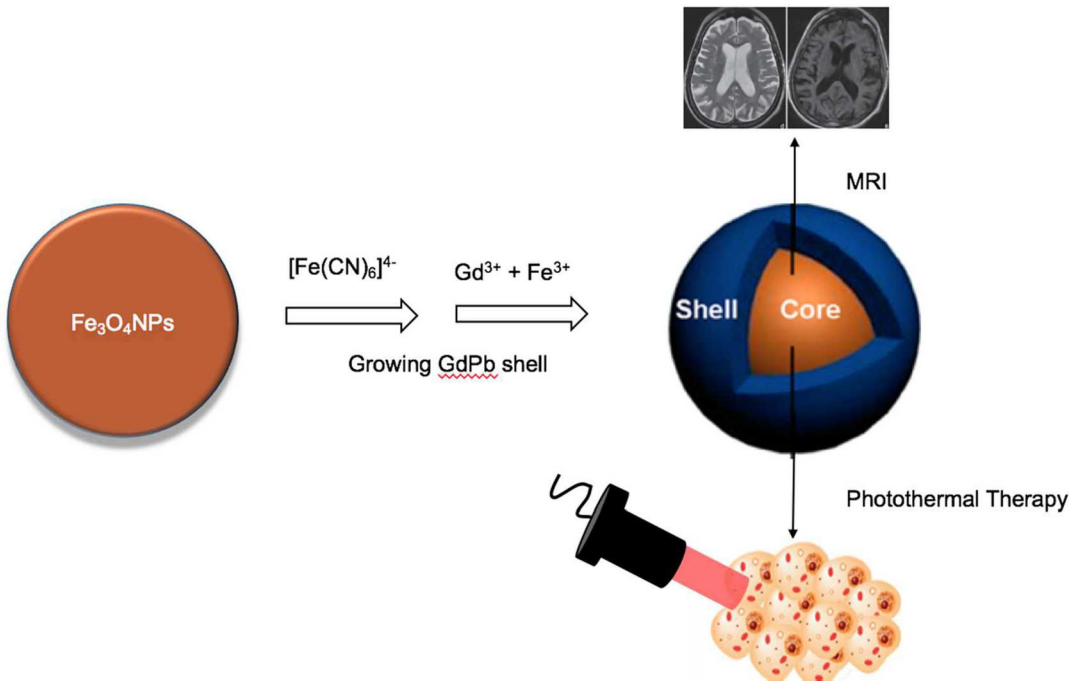

Figure 1: Illustration of the synthesis procedure and theranostic applications of the multifunctional Fe_3O_4@GdPb NPs.

1.9 Design Goals for Fe_3O_4@GdPb nanoparticles

The objective of this project was to synthesize stable core – shell theranostic nanoparticles that could be used for imaging and therapy using a single platform. We indented to synthesize particles which were between 100 nm to 200 nm nano size range for improved uptake and distribution of the nanoparticles in the tumor. Also, this size range allows the nanoparticles to be cleared away from the circulation. Additionally, the negative charge on the surface of these nanoparticles allows the uptake of the nanoparticles through the cells through either transcytosis across the cell membrane or endocytosis[42]. Moreover, the Prussian blue nanoparticles have the capability of absorbing light at the near infrared region between 650 – 900 nm wavelength, that can penetrate deeper into human tissues[32]. Prussian blue nanoparticles convert this light energy into heat energy causing ablation of tumor cells[32,33]. Gadolinium and iron oxide present in the construct have excellent T1 and T2 – MRI contrast capability, providing radiation free detection of the tumors[39].

1.10 Thesis Outline and Specific Aims

Aim 1: To synthesize and measure the stability of the composite nanoparticles:

The focus of this aim was to synthesize a core of iron oxide and then coat the core with a shell of Gadolinium Prussian blue nanoparticles. Once the synthesis of these nanoparticles was completed an external magnetic field was used to remove all the impurities. The hydrodynamic size of the final nanoparticles was measured using the dynamic light scattering method that determined the hydrodynamic diameter of these

nanoparticles. The charge on the nanoparticles was measured using zeta potential[5-10]. Values of zeta potential were determined using the Smoluchowski diffusion equation[7].

Aim 2: To study the contrast properties of the nanoparticles:

The objective of this aim was study was the effect of the nanoparticles as a MRI contrast agent. We used an 8-channel brain coil to place the phantom in the MRI machine. The phantom was prepared with varying concentrations of the nanoparticles. Different TI and TR measurements were used to measure the correspondent T1 and T2-weighthed images.

Aim 3: To study the effects Fe3O4@GdPb nanoparticles based photo-thermal therapy.

The focus of this aim was to determine the effects of photo-thermal therapy (PTT) on the composite nanoparticles. Additionally, we also studied the effect of PTT on the cells using the nanoparticles.

Aim 4: To study the biosafety of the nanoparticles.

The goal of this aim was to study the biosafety of these nanoparticles, by placing the nanoparticles along with with Neuroblastoma neuro2a cells for 24-hours. Later the cytotoxicity of these cells was measured using a CellTiter Glo-assay.

Chapter 2: METHODS

2.1 Materials

The ultrapure water used for all the synthesis procedures was obtained from a Millipore Milli-Q system with a resistivity of at least 17.8 MΩ -cm. Reagents and chemicals used were all purchased from Sigma-Aldrich or ThermoFisher Scientific and used without further purification[5,6,10].

2.2 Iron oxide Gadolinium Prussian blue nanoparticles synthesis (Fe_3O_4@GdPb):

2.2.1 Iron oxide nanoparticles synthesize

The core of these composite nanoparticles consist of iron oxide nanoparticles. We used the most conventional method of co-precipitation for synthesizing Fe_3O_4 nanoparticles[5,16]. To synthesize the iron oxide nanoparticles, Iron (II) chloride tetrahydrate (ferric) and Iron (III) chloride hexahydrate (ferrous) ions were added in a 1:2 molar ratios. This mixture was then added dropwise to sodium hydroxide (NaOH, 5M) solution[5,6]. Using an external magnetic field all the impurities were removed and the nanoparticles were later diluted to the desired concentration (1mg mL-1).

2.2.2 Synthesis of Fe_3O_4@GdPb nanoparticles

The iron oxide nanoparticle cores were added dropwise to a potassium hexacyanoferrate (II) trihydrate [$K_4Fe(CN)_6.3H_2O$] at 50^o C, 2 mM at a pH = 3 in a sonicator bath[6]. Next this solution was added to mixture of iron (III) chloride hexahydrate ($FeCl_3$) and gadolinium (III) nitrate ($Gd(NO_3)_3$) at a pH = 3 and 2 mM in a sonicator bath with continuous stirring at 50^o C. The aqueous solution that was formed was subjected thrice

to an external magnetic field to remove all the impurities and was finally diluted in Milli-Q water to obtain a concentration of 1 mg/ml^{-1}

2.3 Fe_3O_4@GdPb Nanoparticles Stability Measurements

The hydrodynamic size of the composite nanoparticles was measured using dynamic light scattering (DLS) as a function of time. We aimed to synthesize these nanoparticles in the range of 100 nm – 200 nm as this particle size range has the ability to entire into the body circulation and invade the tumor vasculature[24]. The zeta potentials all the nanoparticles was measured using a Zetasizer Nano ZS (Malvern Instruments, Worcestershine, U.K.)[36]. The size of the nanoparticles was measured over a period of 5 days. The Vis-NIR absorbance spectra of the nanoparticles were measured using the VISIONlite software on the Genesys 10S spectrophotometer (Thermo Scientific, Waltham, MA). A 10µg/mL of the nanoparticles dispersed in Milli-Q water was used to measure the size, zeta potential and Vis-NIR absorbance of these nanoparticles. The software used to measure the mean hydrodynamic size of the nanoparticles is Zetasizer Nano ZS (Malvern Instruments, Worcestershire, U.K.).

2.4 Transmission Electron Microscopy (TEM)

TEM was performed on a JEM-2100 FEG high- resolution transmission electron microscope at 200kV. A 10 uL of Fe_3O_4@GdPb at 1mg mL^{-1} nanoparticles was dropped on a formvar grid with 100 mesh (obtained from Electron Microscopy Sciences). Energy-dispersed X-ray spectroscopy (EDS) was performed with an Oxford Instruments INCA 250 system coupled to the TEM microscope. The EDS measurement helped us to

obtain insight regarding percentages of the atomic weight and overally weight of the components in the composite nanoparticles[18,20]. A total of 7 scans were performed on different parts of the sample and then averaged to give relative atomic percentage of gadolinium, iron, potassium, chlorine and oxygen.

2.5 Magnetic Resonance Imaging (MRI) Phantom

The Fe_3O_4@GdPb nanoparticle relativities were performed using a GE 3.0T Magnetic Resonance Imaging machine. The nanoparticles were prepared with varying concentrations obtained by serial dilution starting with a concentration of 0.4 mg/mL^{-1} in a 96 well plates in 0.5% agarose solutions[23-26]. The Fe_3O_4@GdPb nanoparticles were compared gadolinium Prussian blue nanoparticles for the T1 – weighted MRI sequences and with the iron oxide for the T2- weighted MRI sequences. An 8-channel brain coil was used to place the phantom for the MRI images. A constant temperature of 23ºC was maintained for all the measurements. The phantom was placed on a 2% solid block of agar and secured using an 8 channel HD brain coil and tape. T_1 and T_2 relaxation times were measured in the same coronal 0.5mm thick slice. The inversion time (TI) was varied to obtain T_1 measurements (T_1 = 50ms – 4000ms)[10]. To obtain T_2 measurements we obtained images while varying repetition time(TR) ($T_2$12ms – 245ms). OsiriX was used to analyze the signal intensity within the region of interest (ROI) of the acquired images. To measure the T_1 inversion, the signal intensity was plotted against the TI and TE for the T_2 decay curves. The data was then fitted using the following equation[5,6,7]:

$$T_1\text{: } (TR) = A\,(1 - e^{(-TR/T1)}) + y_o \qquad \ldots (1)$$

$$T_2: (TE) = A\,(1 - e^{(-TE/T2)}) + y_o \qquad \ldots (2)$$

The innate behavior of the nanoparticles as contrast agents when subjected to magnetic field, R_1 and R_2 relaxation, rates can be obtained from $1/T_1$ and $1/T_2$ respectively[59].

2.6 In vitro Photothermal therapy on the Fe_3O_4@GdPb Nanoparticles

To study the photothermal therapy of the Fe_3O_4@GdPb nanoparticles, aqueous dispersions of the nanoparticles were exposed to a laser with the wavelength of 808nm (NIR). We investigated the photothermal heating capabilities as a function of concentration of the nanoparticles and as a function of output power. Photothermal therapy can cause rapid loosening of cell membranes and denaturing of the proteins in turn damaging the tumor cells[24,26,28]. In-vitro photothermal therapy studies were performed using an 808nm NIR laser from Laserglow Technologies (Toronto, ON, Cananda). The nanoparticles at a concentration of 1.0 mg ml^{-1} were subjected to varying laser power. To study the PTT effect as a function of concentration, varying the concentration of the theranostic nanoparticles from 0.01 mg mL^{-1} to 0.2 mg mL^{-1} were irradiated at 1.875Wcm^{-2} for 10mins[6.7]. We also studied the cyclic heating and cooling of the nanoparticles to investigate the stability of the nanoparticles as a photothermal agent using photothermal conversion efficiency. This also allows us to fine tune the laser power, exposure time and concentration to obtain optimal heating without causing damage to the surrounding healthy tissues[37].

2.7 Fe_3O_4@GdPb nanoparticles cytotoxicity studies

Murine Neuroblastoma cell line Neuro2a cells were originally obtained from American Type Culture Collections (ATCC) and cultured under recommended conditions. Cells were cultured in EMEM (ThermoFisher, CA) containing 10% fetal bovine serum (ThermoFisher, CA) and 1% penicillin streptomycin (Sigma Aldrich, St. Louis, MO).

Fe_3O_4@GdPb nanoparticles suspended in Milli-Q water were co-incubated with the Neuro2a cells in vitro. Cell viability after incubation with the degradation products was measured using a cell Titer-Glo viability assay (Promega) as per the manufacturer's protocol that determined the number of viable cells in the culture based on quantitation of the ATP present, which signals the presence of metabolically active cells[10]. The viabilities were measured after incubating the cells with the nanoparticles for 24 hours[12-15]. These studies were performed to investigate the ideal concentration at which the nanoparticles are not toxic to the cells. To study the effect functionality of the nanoparticles as a photothermal agent with cells, 5,000 cells mL^{-1} of neuro2a cells were incubated with varying concentration of Fe_3O_4@GdPb nanoparticles (0.01mg/ml, 0.05mg/ml and 0.1mg/ml) in a 96 well plate. Laser beam (1.5 W cm^{-2}, 808nm, 10 mins) was used to irradiate the cells growing on the bottom of the well plates. The cytotoxicity of the treated cells was then measured after 24 hours using the cellTiter-Glo assay. The amount of ATP is directly proportional to the number of cells alive in the culture. This experiment provided the idea concentration which could be used for the treatment of the cancer cells.

Chapter 3: RESULTS AND DISCUSSION

3.1 Stability and Absorbance Properties of the Nanoparticles

We measured the size and stability of the composite nanoparticles using dynamic light scattering measurements (DLS) to demonstrated that the mean hydrodynamic diameter (Figure 1A) of the Fe_3O_4@GdPb nanoparticles is 150 nm compared to 90 nm Fe_3O_4 nanoparticles and for 55 nm to Gadolinium Prussian blue was[5,6,36]. Hence this proves that we could synthesize composite nanoparticles that were within the nanometer dimensions. We conducted studies to determine the stability of the composite nanoparticles over a period of 5 days. Using DLS, we observed the Fe_3O_4@GdPb nanoparticles to exhibit constant sizes within a range of 150 nm to 180 nm (Figure 1B). After injecting the nanoparticles remain in the body circulation for a few hours, therefore, the increasing size of these composite nanoparticles over several days is not of significant concern[14,15,17]. The Vis-NIR spectrum of nanoparticles (Figure 1C) demonstrated its characteristic absorption band from 650-900nm, corresponding to the energy of the metal-to-metal charge transfer between Fe^{II} and Fe^{III} through the cyanide bridge of the PBNP lattice (λmax = 705 nm). This is important as the near infrared region absorbance allows greater depth of tissue penetration of the NIR laser beneath the skin triggering photothermal heating[7,22,23]. The zeta potential of the composite nanoparticles demonstrated the charge on the Fe_3O_4@GdPb nanoparticles which was -16.56 mV compared to the charges on Fe_3O_4 nanoparticles which was -13.2 mV and GdPb nanoparticles was -24.8 mV (Figure 1D). This shows that the nanoparticles lie in a range between the two composite

nanoparticles which form the nano-shell and the nano-core. Additionally, the negative charge allows deeper penetration of the nanoparticles within the tumor[16].

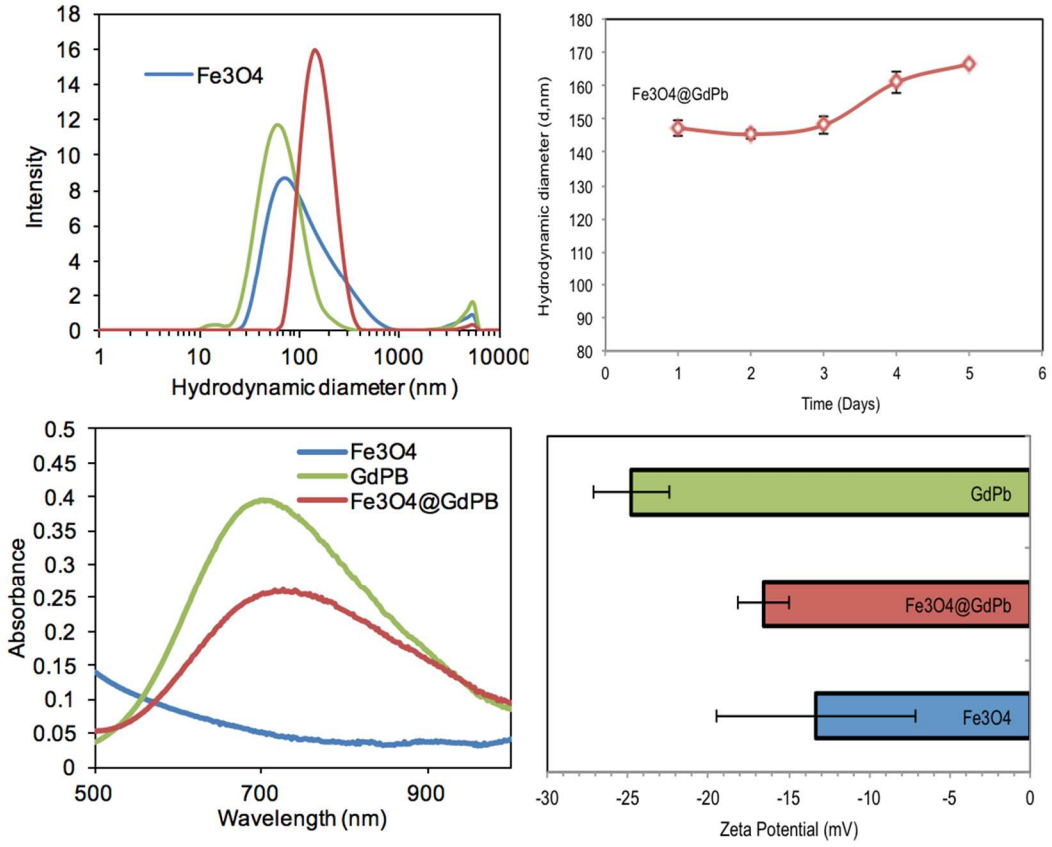

Figure 2: Characterization of Fe_3O_4@GdPb nanoparticles (A) Size distribution of the Fe_3O_4@GdPb (blue), Fe_3O_4(blue) and GdPb (green) nanoparticles measured by dynamic light scattering. (B) Multi-day stability of the Fe_3O_4@GdPb nanoparticles. (C) UV-vis absorption spectra of Fe_3O_4@GdPb, Fe_3O_4 and GdPb nanoparticles showed near infrared absorbance from 650-900nm of Fe_3O_4@GdPb nanoparticles. (D) Zeta potential of Fe_3O_4@GdPb, Fe_3O_4 and GdPb nanoparticles.

3.2 Transmission Electron Microscopy (TEM)

The size and morphology of individual Fe_3O_4@GdPb nanoparticles were confirmed by TEM. These images gave us a clear crystal pictures of the composite nanoparticles. The chemical composition of the material was confirmed by energy-dispersive X-ray spectroscopy (EDS) over the areas covered by the NPs and by elemental analysis[7]. The elemental analysis indicated the concentration of the gadolinium and iron in the nanoparticles. These concentrations were important as these two components have the properties for MRI contrast. The elemental analysis indicated 7.33 weight percentage of gadolinium and 16.13 weight percentage of iron components within the nanoparticles. The EDS gave the insight of the total percentage of the weight and atomic weight of the components in the Fe_3O_4@GdPb nanoparticles. (Figure 3B).

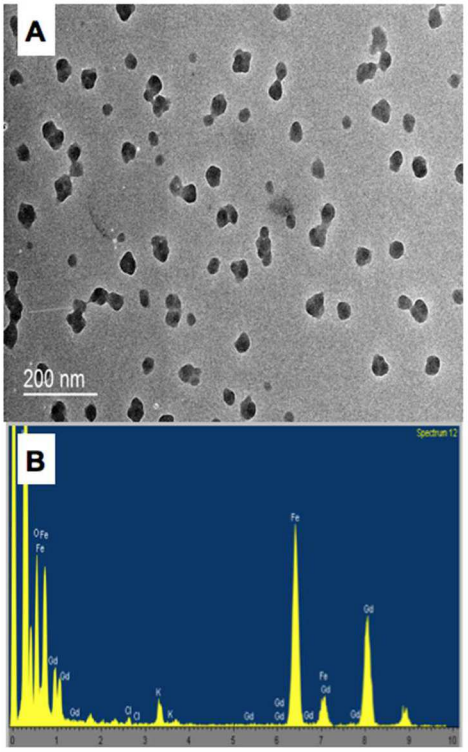

Element	Weight %	Atomic %
Fe	16.13	5.76
Gd	7.33	0.925

Figure 3: Physical and chemical characterization of the nanoparticle core. (A) Representative TEM images of the Fe3O4@GdPb nanoparticles (Scale bar = 0.5µm) (B) EDS spectrum of the composition is derived by the built-in software (INCA, Oxford Instruments, UK) from the attribution of electronic energies profile for Fe and Gd.

3.3 Magnetic Resonance Imaging Relaxation Time Measurements

Magnetic properties of the Fe_3O_4@GdPb nanoparticles were also studied. The generation of both T1 and T2 may be explained by contributions from two relaxation mechanisms. First, the contribution of protons, from coordinated or interstitial water molecules located

in the particles, interacting with gadolinium cations through an inner-sphere mechanism gives positive contrast in T1 - weighted images[6]. Second, the presence of iron in the core of the composite nanoparticles increases the overall spin density and the magnitude of the paramagentism of the nanoparticles was confirmed by magnetometry studies[10,11]. The presence of paramagnetic particles distributing the local magnetic field in its vicinity generates negative contrast (hypointensity) in T2 – weighted images[10]. The capability to generate hyper- and hypointensity with the same contrast agent is highly desirable when trying to increase the relative contrast sensitivity by image subtraction or to obtain T1 and T2 – weighted images with unique contrast[10-15]. The relaxation rates obtained were plotted against the concentration of the corresponding contrast agents, iron and gadolinium respectively.

We determined the longitudinal and transverse relaxivitieis (r1 and r2 values respectively) of the nanoparticles at a magnetic field of 3T using serial dilution (Figure A). The longitudinal (r1) and transverse (r2) relaxivities are derived from linear fits of R1 and R2 versus gadolinium and iron concentration respectively[36]. Using Gadolinium Prussian Blue nanoparticles as a control, a small increase in the brightening effect was observed with the increase in the concentration of the nanoparticles. The contrast was compared to the relaxivity of commercial gadolinium chelate formulation (Magnevist), intravenous contrast agent available for clinical use[16]. Using iron oxide nanoparticles as a control, an increasingly darkening effect was observed in the T1- weighted magnetic resonance images. Figure 4B, C, shows the T1 relaxation rate (1/T1) as a function of the gadolinium concentration in the Fe_3O_4@GdPb nanoparticles. The weighted transverse

relaxivity value (r_1) was measured to be 5.5 mM^{-1} s^{-1}. Also, figure 4D,E shows the T2 relaxation rate (1/T2) as a function of the iron concentration in the composite nanoparticles. The weighted transverse relaxivity value (r_2) was measured to be 126.01 Mm^{-1} s^{-1} which is a good value.

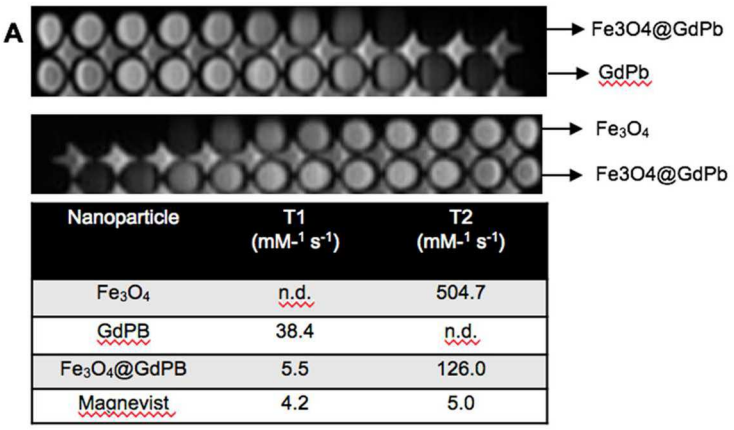

Nanoparticle	T1 (mM^{-1} s^{-1})	T2 (mM^{-1} s^{-1})
Fe_3O_4	n.d.	504.7
GdPB	38.4	n.d.
Fe_3O_4@GdPB	5.5	126.0
Magnevist	4.2	5.0

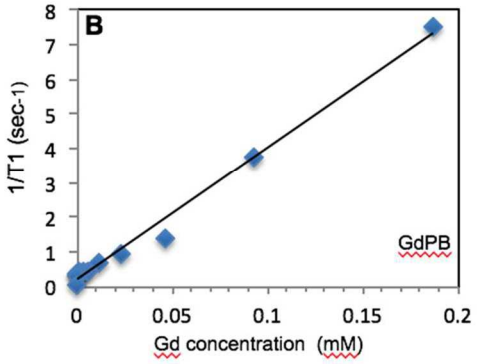

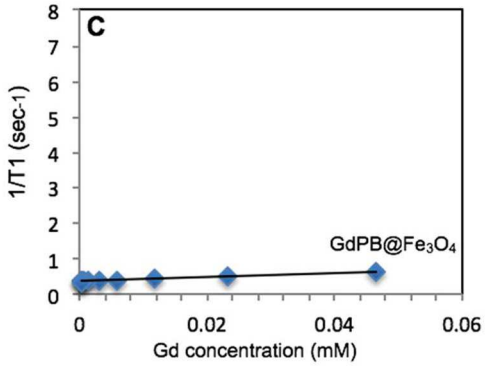

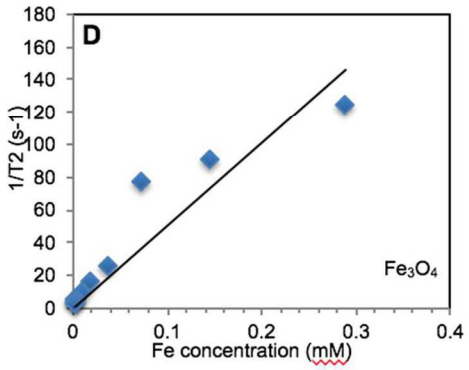

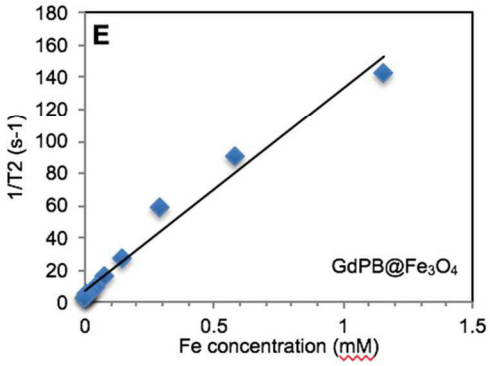

Figure 4: (A) Representative pictures of the phantoms used for determination of T1 and T2 weighted images respectively. (B) R_1 in sec plotted against the gadolinium concentration of the nanoparticles for GdPb. (C) R_1 in sec plotted against the gadolinium concentration of the nanoparticles for Fe_3O_4GdPb. (D) R_2 in sec plotted against the iron oxide concentration of the Fe_3O_4 nanoparticles. (E) R_2 in sec plotted against the iron oxide concentration of the Fe_3O_4@GdPb nanoparticles

3.4 Photothermal Capabilities of the Composite Nanoparticles:

Next, we wanted to study the heating capabilities of the nanoparticles. The Prussian blue (PB) nanoparticles when irradiated by an 808 nm near infrared (NIR), the near absorbing PB NPs are photothermally heated as they have the capability of converting light energy at the Vis-NIR region into heat energy[19]. Hence, we wanted to study if these composite nanoparticles retain similar photothermal heating properties. The heating capabilities of these nanoparticles were examined as a function of concentration and laser power. It was observed that, with increasing concentration of the nanoparticles, the heating was increased. Further, the PTT is also dependent on the laser power and with the increase in the laser power increasing the heating of the nanoparticles. To demonstrate this, we irradiated 0.1mg mL^{-1} of Fe_3O_4@GdPb nanoparticles with different laser powers from 0.625 Wcm^{-2} to 3.125 Wcm^{-2}. Additionally, we exhibited the stability of Fe_3O_4@GdPb nanoparticles as a photothermal agent through cyclic heating experiment. The Fe_3O_4@GdPb nanoparticles showed consistent heating and cooling over four heating and cooling cycle. Hence this proved that the heating of these nanoparticles can be controlled

as a function of concentration of the nanoparticles and laser power. Also, at a given constant laser power and constant concentration these composite nanoparticles are stable photothermal agents.

3.5 Photothermal Conversion Efficiency:

The photothermal conversion efficiency of the nanoparticles allows us to allows to fine tune the laser power, laser exposure time, and concentration to obtain optimal heating to avoid damage to the surrounding healthy cells[24]. We performed photothermal conversion efficiency on the nanoparticles to learn more about the Fe_3O_4@GdPb nanoparticles as a photothermal agent. This was performed by irradiating 0.1mg mL^{-1} of nanoparticles with an 808 nm laser at 1.8W. After a stabilized temperature was obtained the laser was turned off and the decrease in temperature was measured. To obtain the photothermal conversion efficiency we use the model described by Roper et al[7].

$$\eta_T = \frac{hA(T_{max} - T_{amb}) - Q_0}{I(1 - 10^{-A_\lambda})}$$

where h is the heat transfer coefficient, A is the surface area of heat transfer of the system, Tmax is the maximum system temperature, Tamb is the ambient temperature, Q0 is the rate of heat input due to absorption of light energy by water, I is the laser power, and Al is the absorbance of the PB NPs at 808nm).

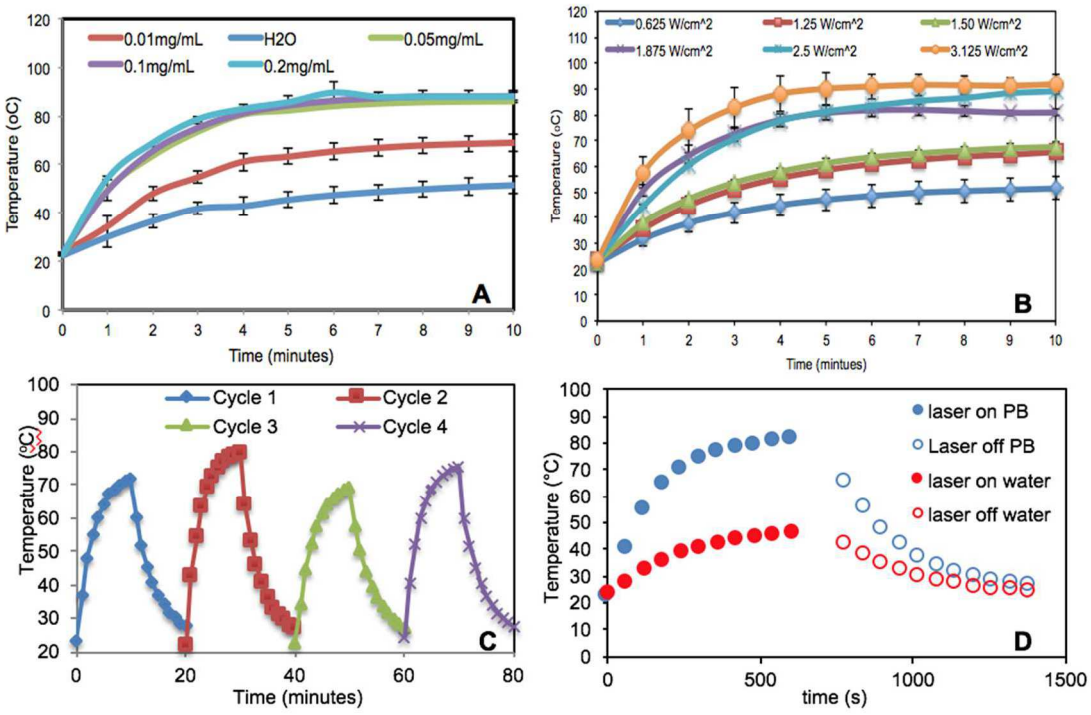

Figure 5: Photothermal heating characteristics of Fe_3O_4@GdPb nanoparticles (A) Photothermal heating of varying concentration of the nanoparticles with constant laser power of 1.875 W/cm^2 for 10 mins (B) Photothermal heating of 1mg mL^{-1} using varying 808 nm NIR laser power (0.625-3.75 W cm^{-2}) for 10 mins (C) Temperature profiles during cyclic heating of 1mg mL^{-1} composite nanoparticles using an 808 nm NIR laser (laser on/off time: 10min) (D) Photothermal Conversion efficiency of Fe_3O_4@GdPb = 16.1%

3.6 In-Vitro Capabilities of Fe_3O_4@GdPb Nanoparticles

To study the biosafety and functionality of the theranostic nanoparticles we performed cytotoxicity studies. We examined the biocompatibity of these composite nanoparticles

with the neuro2a cells, a mouse neuroblastoma cell line. The cytotoxicity was measured after 24 hours using the cellTiter-Glo viability assay. Varying concentration of nanoparticles were co-incubated with 10,000 seeded cells of neuro2a. There was no apparent change in cell viability in the concentration range below 0.1 $mg.mL^{-1}$ indicating reliable biocompatibity of the composite nanoparticles. Future, to evaluate the photothermal therapeutic effect of the nanoparticles, Neuro2a cells were incubated with the nanoparticles in a 96-well plate were irradiated with a laser (808 nm, 1.5 $W.cm^{-2}$, 10 min). After 24 hours the cytotoxicity of the nanoparticles was measured using a cellTiter- Glo assay. As no cell death was observed in the presence of a low concentration of the nanoparticles (0.02 $mg.mL^{-1}$) since the temperature elevation was not sufficient to kill the cancer cells. On the contrary, with the increase in the concentration of the nanoparticles the temperature elevation was sufficient to cause irradiation of the cells. These results prove, when the cells are in contact with the theranostic nanoparticles the cells viability does not significantly hence suggesting that the nanoparticles are biocompatible with the cells. On the other hand, when the laser power (808 nm, 1.5 $W.cm^{-2}$, 10 mins) was added along with the nanoparticles, cell viability decreased.

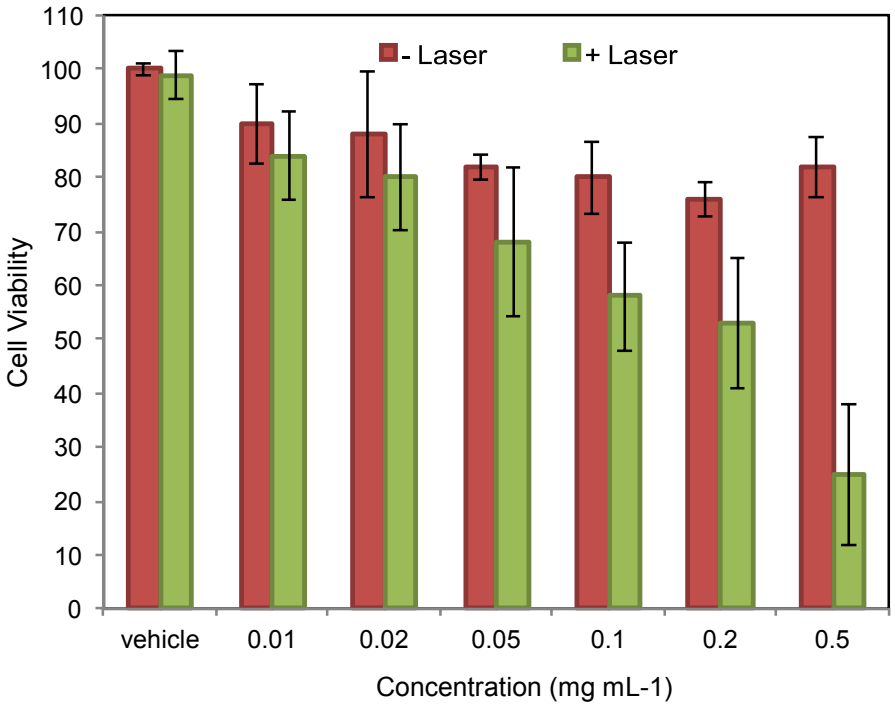

Figure 6: Cytotoxicity of Fe3O4@GdPb nanoparticles with varying concentration of the composite nanoparticles added to a fixed number of Neuroblastoma (neuro2a) cells in-vitro (red) and after performing photothermal therapy on the cells (green) using an 808nm laser power.

3.7 Summary

Hence, these results prove we could synthesize stable theranostic nanoparticles by growing a gadolinium Prussian blue nanoshell around a superparamagnetic iron oxide nanocore. The obtained Fe_3O_4@GdPb nanoparticles show promising radiation free detection results as an MRI contrast agent with both T1 and T2 – weighted sequences. Also these nanoparticles demonstrate excellent as photothermal properties at the near

infrared region. Thus these theranostic nanoparticles permit less invasive and more precise cancer treatment. These also allow MRI guided photothermal therapy.

Chapter 4: CONCLUSION

4.1 Summary

In this paper we have described the synthesis and evaluation of magnetic Prussian blue nanoparticles (Fe_3O_4@GdPb) for the potential use as a theranostic agent. These composite nanoparticles can be simultaneously used for enhanced magnetic resonance imaging (MRI) as well as for laser induced photothermal therapy for treating neuroblastoma cancers. These nanoparticles combine the capabilities of MRI contrast agent and photothermal therapy. This allows us to synthesize nanoparticles for efficient MRI- guided photothermal therapy. Our results showcase the potential for the use of these composite nanoparticles for MRI imaging in combination with ablating the tumor cells as a treatment and detection of advanced cancer tumors using a single platform.

4.2 Contribution to the Field

This project utilizes the advantages of iron oxide nanoparticles as a T2 MRI contrast agent along with the combination of gadolinium present in the shell that are excellent T1 contrast agent for MRI and Prussian blue nanoparticles for photothermal therapy. Our rationale for pursuing photothermal therapy in tumor therapy is based on the extensive literature demonstrating the reduced heat tolerance of tumors in comparison to the normal cells[6-7]. The use of the NIR light is advantageous on account of its extensive safety profile in disease diagnostics and therapy[50-55]. The other advantage with these nanoparticles is that they are very low cost and easy to synthesized. These composite nanoparticles provide efficient MRI guided photothermal therapy using a specialized lone platform.

4.3 Future Studies

All the studies described have helped prove that composite nanoparticles can be used for theranostic applications in cancer therapy. These nanoparticles have the advantage that they are easy to synthesize and are FDA approved[43]. In the next project we would evaluate the application of these nanoparticles in an animal model. This would provide a clear idea about the function of the nanoparticles when in contact with a biological environment. Later, MRI imaging and photothermal therapy would be performed using these theranostic nanoparticles in the animals[46-49]. These nanoparticles could also be used for magnetic hyperthermia using a rapidly alternating magnetic field to studies to increase the uptake of the anti cancer agents at the tumor site[59-62]. Finally, another area of research would be to biofunctionalize the Fe_3O_4@GdPb nanoparticles with antibodies for targeting the nanoparticles to site of interest.

Chapter 5: Bibliography

1) "What Is Cancer?" *National Cancer Institute*. NIH, n.d. Web. 10 Apr. 2016.

2) Siegel, R. L.; Miller, K. D.; Jemal, A., Cancer statistics, 2015. CA Cancer J Clin 2015, 65 (1), 5-29.

3) Bellanti, F.; Kågedal, B.; Della Pasqua, O., Do pharmacokinetic polymorphisms explain treatment failure in high-risk patients with neuroblastoma? Eur J Clin Pharmacol 2011, 67 Suppl 1, 87-107.

4) Barros ALB, Soares DCF (2014) Theranostic Nanoparticles: Imaging and Therapy Combined. J Mol Pharm Org Process Res 2:e113. doi: 10.4172/2329-9053.1000e113

5) Fu, Guanglei, et al. "Magnetic Prussian blue nanoparticles for targeted photothermal therapy under magnetic resonance imaging guidance."*Bioconjugate chemistry* 25.9 (2014): 1655-1663.

6) Dumont, Matthieu F., et al. "Biofunctionalized gadolinium-containing Prussian blue nanoparticles as multimodal molecular imaging agents." *Bioconjugate chemistry* 25.1 (2013): 129-137.

7) Hoffman, Hilary A., et al. "Prussian blue nanoparticles for laser-induced photothermal therapy of tumors." *RSC Advances* 4.56 (2014): 29729-29734.

8) Dumont, Matthieu F., et al. "Manganese-containing Prussian blue nanoparticles for imaging of pediatric brain tumors." *International journal of nanomedicine* 9 (2014): 2581.

9) Morana, G., Salviato, E., and Guarise, A. (2007) Contrast agents for hepatic MRI. Cancer Imaging 7, S24−27.

10) Korkusuz, H., Ulbrich, K., Welzel, K., Koeberle, V., Watcharin, W., Bahr, U., Chernikov, V., Knobloch, T., Petersen, S., Huebner, F., Ackermann, H., Gelperina, S., Kromen, W., Hammerstingl, R.,Haupenthal, J., Gruenwald, F., Fiehler, J., Zeuzem, S., Kreuter, J.,Vogl, T. J., and Piiper, A. (2013) Transferrin-coated gadolinium nanoparticles as MRI contrast agent. Mol. Imaging Biol. 15, 148−154.

11) Broz, P., Ben-Haim, N., Santini, F., Marsch, S., Scheffler, K., Meier, W., and Hunziker, P. (2009) Nano imaging technologies: polymer vesicles loaded with precipitated gadolinium nanoparticles: a novel target-specific contrast agent for magnetic resonance imaging Eur. J. Nanomedicine 2, 3−49.

12) Catala, L., Brinzei, D., Prado, Y., Gloter, A., Stéphan, O., Rogez, G., and Mallah, T. (2009) Core−multishell magnetic coordination nanoparticles: toward multifunctionality on the nanoscale. Angew. Chem., Int. Ed. 48, 183−187.

13) Hou, S., Tong, S., Zhou, J., and Bao, G. (2012) Block copolymer-based gadolinium nanoparticles as MRI contrast agents with high T1 relaxivity. Nanomedicine 7, 211−218.

14) J. Li, F. Jiang, B. Yang, X. Song, Y. Liu, H. Yang, D. Cao, W. Shi and G. Chen, Sci. Rep., 2013, 3, 1–7.

15) G. M. Brodeur, M. D. Hogarty, Y. P. Mosse and J. M. Maris, Principles and Practice of Pediatric Oncology, ed. P. A. Pizzo and D.G. Poplack, Wolters Kluwer Health/Lippincott Williams & Wilkins, Philadelphia, 6th edn, 2010, pp. 886–922.

16) G. Fu, W. Liu, S. Feng and X. Yue, Chem. Commun., 2012, 48 11567–11569.

17) M. Chu, Y. Shao, J. Peng, X. Dai, H. Li, Q. Wu and D. Shi, Biomaterials, 2013, 34, 4078–4088.

18) Meng, F.; Cheng, R.; Deng, C.; Zhong, Z., Intracellular drug release nanosystems Materials Today 2012, 15, 436-442.

19) Schoenborn, J. R.; Wilson, C. B., Regulation of interferon-gamma during innate and adaptive immune responses. Adv Immunol 2007, 96, 41-101.

20) Itaya, K.; Akahoshi, H.; Toshima, S., Electrochemistry of Prussian Blue Modified Electrodes: An Electrochemical Preparation Method. J Electrochem Soc 1982, 129 (7),1498-1500.

21) Song, C., RobertPark, Heon Joo, Influence of Tumor pH in Therapeutic Response. In Cancer Drug Discovery and Development: Cancer Drug Resistance, Inc., B. T. H. P., Ed. Totowa, NJ, 2006; pp 21-42.

22) Itaya, K.; Akahoshi, H.; Toshima, S., Electrochemistry of Prussian Blue Modified Electrodes: An Electrochemical Preparation Method. J Electrochem Soc 1982, 129.

23) Ascierto, P. A.; Marincola, F. M.; Ribas, A., Anti-CTLA4 monoclonal antibodies: the past and the future in clinical application. J Transl Med 2011, 9, 196.

24) Fu, G.; Liu, W.; Feng, S.; Yue, X., Prussian blue nanoparticles operate as a new generation of photothermal ablation agents for cancer therapy. Chem Commun 2012.

25) Durymanov, M. O.; Rosenkranz, A. A.; Sobolev, A. S., Current Approaches for Improving Intratumoral Accumulation and Distribution of Nanomedicines. Theranostic 2015, 5 (9), 1007-20.

26) Cobley, C. M.; Au, L.; Chen, J.; Xia, Y., Targeting gold nanocages to cancer cells for photothermal destruction and drug delivery. Expert Opin Drug Deliv 2010, 7 (5).

27) Hirsch, L. R.; Stafford, R. J.; Bankson, J. A.; Sershen, S. R.; Rivera, B.; Price, R. E.; Hazle, J. D.; Halas, N. J.; West, J. L., Nanoshell-mediated near-infrared thermal therapy

of tumors under magnetic resonance guidance. Proc Natl Acad Sci USA 2003,100 (23), 13549-54.

28) Wang, C.; Xu, L.; Liang, C.; Xiang, J.; Peng, R.; Liu, Z., Immunological responses triggered by photothermal therapy with carbon nanotubes in combination with anti-CTLA-4 therapy to inhibit cancer metastasis. Adv Mater 2014, 26 (48), 8154-62.

29) Tao, Y.; Ju, E.; Liu, Z.; Dong, K.; Ren, J.; Qu, X., Engineered, self-assembled near-infrared photothermal agents for combined tumor immunotherapy and chemophotothermal therapy. Biomaterials 2014, 35 (24), 6646-56.

30) Tao, Y.; Ju, E.; Ren, J.; Qu, X., Immunostimulatory oligonucleotides-loaded cationic graphene oxide with photothermally enhanced immunogenicity for photothermal/immune cancer therapy. Biomaterials 2014, 35 (37), 9963-71.

31) Wu, F.; Zhou, L.; Chen, W. R., Host antitumour immune responses to HIFU ablation. Int J Hyperthermia 2007, 23 (2), 165-71.

32) Yang, Y.; Faustino, P. J.; Progar, J. J.; Brownell, C. R.; Sadrieh, N., et al., Quantitative determination of thallium binding to ferric hexacyanoferrate: Prussian blue. Int J Pharm 2008, 353 (1-2), 187-94.

33) Cui, J.; Wang, N.; Zhao, H.; Jin, H.; Wang, G.; Niu, C.; Terunuma, H.; He, H.; Li, W., Combination of radiofrequency ablation and sequential cellular immunotherapy improves progression-free survival for patients with hepatocellular carcinoma. Int J Cancer 2014, 134 (2), 342-51.

34) Lal, S.; Clare, S. E.; Halas, N. J., Nanoshell-enabled photothermal cancer therapy impending clinical impact. Acc Chem Res 2008, 41 (12), 1842-51.

35) Dewhirst, M. F., JrRoemer RB, Hyperthermia. Gunderson LL, Tepper JE: New York,

2000.

36) Vojtech, J. M.; Cano-Mejia, J.; Dumont, M. F.; Sze, R. W.; Fernandes, R., Biofunctionalized prussian blue nanoparticles for multimodal molecular imagin applications. J Vis Exp 2015, (98), e52621.

37) Chekina, N., Horák, D., Jendelová, P., Trchová, M., Beneš, M. J., Hrubý, M., Herynek, V., Turnovcová, K., and Syková, E. (2011) Fluorescent magnetic nanoparticles for biomedical applications. J.Mater. Chem. 21, 7630−7639.

38) Broz, P., Ben-Haim, N., Santini, F., Marsch, S., Scheffler, K., Meier, W., and Hunziker, P. (2009) Nano imaging technologies polymer vesicles loaded with precipitated gadolinium nanoparticles: a novel target-specific contrast agent for magnetic resonance imaging. Eur. J. Nanomedicine 2, 3−49.

39) Hou, S., Tong, S., Zhou, J., and Bao, G. (2012) Block copolymer-based gadolinium nanoparticles as MRI contrast agents with high T1 relaxivity. Nanomedicine 7, 211−218.

40) Shokouhimehr, M., Soehnlen, E. S., Hao, J., Griswold, M., Flask, C., Fan, X., Basilion, J. P., Basu, S., and Huang, S. D. (2010) Dual purpose prussian blue nanoparticles for cellular imaging and drug delivery: a new generation of T1 weighted MRI contrast and small molecule delivery agents. J. Mater. Chem. 20, 5251−5259.

41) Bulte, J. W. M., and Kraitchman, D. L. (2004) Iron oxide MR contrast agents for molecular and cellular imaging. NMR Biomed. 17, 484−499.

42) Morana, G., Salviato, E., and Guarise, A. (2007) Contrast agents for hepatic MRI. Cancer Imaging 7, S24−27.

43) Liang, G., Ronald, J., Chen, Y., Ye, D., Pandit, P., Ma, M. L., Rutt, B., and Rao, J. (2011) Controlled self-assembling of gadolinium nanoparticles as smart molecular

magnetic resonance imaging contrast agents. Angew. Chem., Int. Ed. 50, 6283−6286.

44) Wojdeł, J. C., and Bromley, S. T. (2006) Band gap variation in prussian blue via cation-induced structural distortion. J. Phys. Chem. B 110, 24294−24298.

45) Korkusuz, H., Ulbrich, K., Welzel, K., Koeberle, V., Watcharin, W., Bahr, U., Chernikov, V., Knobloch, T., Petersen, S., Huebner, F., Ackermann, H., Gelperina, S., Kromen, W., Hammerstingl, R., Haupenthal, J., Gruenwald, F., Fiehler, J., Zeuzem, S., Kreuter, J., Vogl, T. J., and Piiper, A. (2013) Transferrin-coated gadoliniumnanoparticles as MRI contrast agent. Mol. Imaging Biol. 15, 148−154.

46) Uemura, T., Ohba, M., and Kitagawa, S. (2004) Size and surface effects of prussian blue nanoparticles protected by organic polymers. Inorg. Chem. 43, 7339−7345.

47) E. B. Dickerson, E. B. Dreaden, X. Huang, I. H. El-Sayed, H. Chu, S. Pushpanketh, J. F. McDonald and M. A. Elsayed, Cancer Lett., 2008, 269, 57–66.

48) Xie, J.; Lee, S.; Chen, X., Nanoparticle-based theranostic agents. Adv Drug Delivery Rev 2010, 62 (11), 1064-79.

49) Madhusudhan, A.; Reddy, G. B.; Venkatesham, M.; Veerabhadram, G.; Kumar, D. A.; Natarajan, S.; Yang, M. Y.; Hu, A.; Singh, S. S., Efficient pH dependent drug delivery to target cancer cells by gold nanoparticles capped with carboxymethyl chitosan. Int J Mol Sci 2014, 15 (5), 8216-34.

50) Cheng, L.; Gong, H.; Zhu, W.; Liu, J.; Wang, X.; Liu, G.; Liu, Z., PEGylated Prussian blue nanocubes as a theranostic agent for simultaneous cancer imaging and photothermal therapy. Biomaterials 2014, 35 (37), 9844-52.

51) Stern, J. M.; Stanfield, J.; Kabbani, W.; Hsieh, J. T.; Cadeddu, J. A., Selective prostate cancer thermal ablation with laser activated gold nanoshells. The Journal of

urology 2008, 179 (2), 748-53.

52) Durymanov, M. O.; Rosenkranz, A. A.; Sobolev, A. S., Current Approaches for Improving Intratumoral Accumulation and Distribution of Nanomedicines. Theranostics 2015, 5 (9), 1007-20.

53) Zhang, L.; Conejo-Garcia, J. R.; Katsaros, D.; Gimotty, P. A.; Massobrio, M., et al., Intratumoral T cells, recurrence, and survival in epithelial ovarian cancer. N Engl J Med 2003, 348 (3), 203-13.

54) Saboktakin, M. R.; Tabatabaie, R. M.; Maharramov, A.; Ramazanov, M. A., Synthesis and characterization of pH-dependent glycol chitosan and dextran sulfate nanoparticles for effective brain cancer treatment. Int J Biol Macromol 2011, 49 (4), 747-51.

55) Frangioni, J. V., In vivo near-infrared fluorescence imaging. Curr Opin Chem Biol 2003, 7 (5), 626-34.

56) Rink, J. S.; Plebanek, M. P.; Tripathy, S.; Thaxton, C. S., Update on current and potential nanoparticle cancer therapies. Current opinion in oncology 2013, 25 (6), 646-51.

57) Liu, H., Chen, D., Li, L., Liu, T., Tan, L., Wu, X., and Tang, F. (2011) Multifunctional gold nanoshells on silica nanorattles: a platform for the combination of photothermal therapy and chemotherapy with low systemic toxicity. Angew. Chem., Int. Ed. 50, 891−895.

58) Ma, Y., Liang, X. L., Tong, S., Bao, G., Ren, Q. S., and Dai, Z. F. (2013) Gold nanoshell nanomicelles for potential magnetic resonance imaging, light-triggered drug release, and photothermal therapy. Adv. Funct. Mater. 23, 815−822.

59) Chen, Y. C., Gnyawali, S. C., Wu, F., Liu, H., Tesiram, Y. A., Abbott, A., Towner, R. A., and Chen, W. R. (2008) Magnetic resonance imaging guidance for laser photothermal therapy. J. Biomed.Opt. 13, 044033.

60)http://www.fda.gov/drugs/emergencypreparednes/bioterrorismanddrugpreparedness/ucm130334.htm.

61) Thammawong, C., Opaprakasit, P., Tangboriboonrat, P., and Sreearunothai, P. (2013) Prussian blue-coated magnetic nanoparticles for removal of cesium from contaminated environment. J. Nanopart. Res. 15, 1689.

62) Kievit, Forrest M., and Miqin Zhang. "Cancer nanotheranostics: improving imaging and therapy by targeted delivery across biological barriers."*Advanced Materials* 23.36 (2011).

63) Kievit, Forrest M., and Miqin Zhang. "Surface engineering of iron oxide nanoparticles for targeted cancer therapy." *Accounts of chemical research*44.10 (2011): 853-862.